A Soft-switched isolated Single Stage Bidirectional Three phase AC-DC Converter

Dibakar Das
Department of Electrical Engineering
Indian Institute of Science
Bangalore, India
dibakard@iisc.ac.in

Kaushik Basu
Department of Electrical Engineering
Indian Institute of Science
Bangalore, India
kbasu@iisc.ac.in

***Abstract*—The battery chargers in electric vehicles need to have high efficiency and power density. Moreover, bidirectional power flow capability is necessary for vehicle to grid (V2G) applications. This paper proposes a bidirectional isolated three phase AC-DC converter based on the dual active bridge (DAB) conversion principle and line frequency unfolding resulting in low switching loss. Sections of the fundamental components of line currents are generated using DAB modulation and then appropriately combined to produce the actual line currents. The proposed solution can be used for bidirectional power flow and power factor correction. The high efficiency due to reduced switching loss and improved power density makes it a promising solution for battery chargers particularly in vehicle to grid (V2G) applications.**

***Index Terms*—Dual Active Bridge, Line frequency unfolding**

I. Introduction

Rapidly depleting fossil fuels and the global warming concerns have increased the thrust towards electric vehicle (EV) technologies. Power electronic converters are necessary for interfacing the battery driven electric vehicles to a charging station or the utility grid. On board charging systems should be highly efficient and lightweight so that they do not increase the vehicle weight significantly. Moreover, in vehicle to grid (V2G) applications the converters should have bidirectional power flow capability.

Conventional EV chargers utilize two conversion stages for AC to DC power conversion [1]. The front end is an active hard-switched pulse width modulated (PWM) rectifier which is followed by a DC-DC converter for isolation and voltage matching. The intermediate DC link usually consist of a large and bulky electrolytic capacitor which increases the weight and reduces system reliability. To avert these issues, several works in the literature with single power conversion stage have been reported [2]–[4].

A single stage PWM unidirectional DC-AC converter using line frequency unfolding principle is discussed in [5]. The converter uses a phase shifted full bridge conversion strategy followed by line frequency unfolding. A similar idea based on resonant conversion principle utilizing dual bridge SRC modules is reported in [6]. The topology uses capacitor on the input of the line frequency unfolder to filter the switching ripple components. However, use of series resonant converters results in high losses at light load conditions.

Dual active bridge converters were originally proposed in [7]. Dual active bridge converters offer a promising solution for high power DC-DC converters because of soft switching and bidirectional power flow capability [8]. Several single stage converter solutions have been proposed using the DAB principle. A three phase AC-DC using matrix converter on AC side and H-bridge on DC side is reported in [9]. The converter proposes a modulation strategy which enables soft switching of AC and DC bridges. The proposed modulation strategy results low frequency harmonics in line currents. Moreover, the detailed analysis on soft switching is not provided. A modulation strategy for obtaining open-loop power factor correction and no low frequency current harmonics with the topology in [9] is discussed in [10]. A modulation utilizing push-pull structure on AC side matrix converter and three phase VSI on DC side is reported in [11]. The AC side converter is high frequency switched which results in losses and low efficiency. A modulation strategy utilizing the topology in [9] which achieves primary bridge soft switching is reported in [12]. However, primary bridge zero current switching cannot be guaranteed to be completely lossless.

This paper proposes a novel three phase AC-DC converter topology along with a modulation strategy based on DAB principle. The proposed converter utilizes a line frequency unfolding scheme [6]. The modulation strategy results in soft-switching and line frequency unfolding leads to low switching losses. Moreover, the proposed converter offers a galvanically isolated single stage conversion with bidirectional power flow capability and controllable power factor. Analysis reveals that the DC side H-bridge of the converter is able to achieve soft switching for the entire line cycle which leads to improvement of efficiency. High efficiency and power density of the converter makes it a suitable candidate for on board electric vehicle chargers.

II. Analysis of the proposed Converter

This section describes the proposed converter, modulation strategy and the derivation of important quantities of interest. The proposed converter topology is shown in Fig.1. On the DC side, the H-bridge converter is connected in parallel with primary windings of two high frequency transformer of turns ratio $1 : n$. The inductors L_1 and L_2 are responsible for the

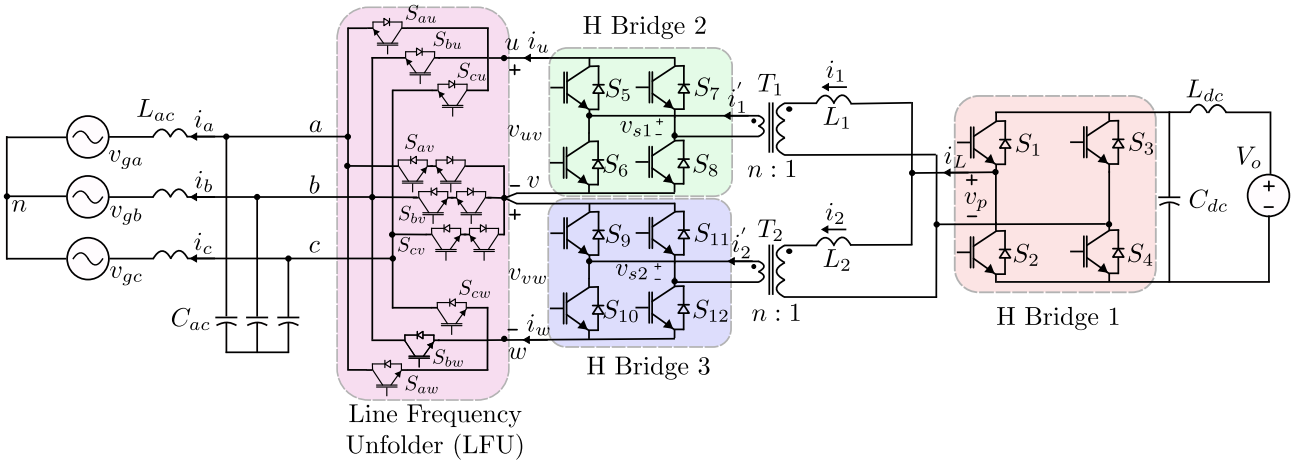

Fig. 1. Proposed DAB based bidirectional converter topology

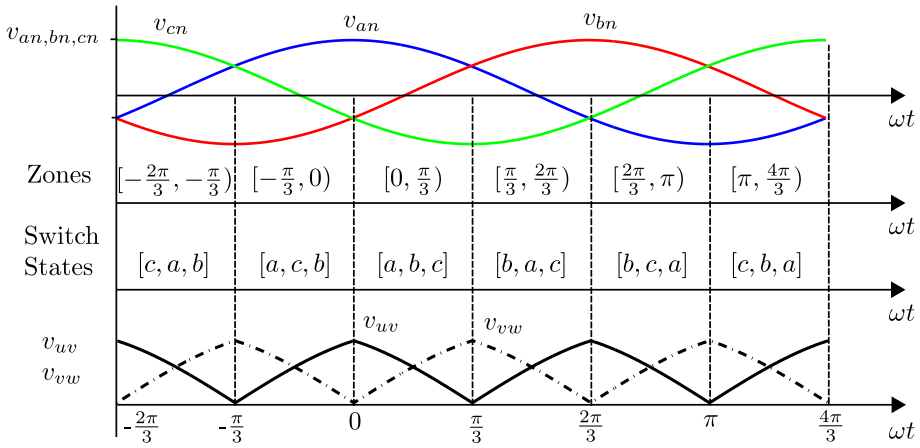

Fig. 2. Waveforms illustrating LFU operation: Line-neutral utility voltages, switching state for each zone and the unfolder output voltages v_{uv} and v_{vw}

TABLE I
DESIGN PARAMETERS OF THE CONVERTER

P	L	n	V_p	V_o	f	f_s	Power Factor
2.1 kW	270μH	0.67	127V	400V	50Hz	20kHz	1.00

power transfer through the DAB principle. These inductors can be the leakage inductance of the transformer or externally connected inductor in series with the transformer. Both the inductors have equal value of inductance L. The AC side windings of the transformers are connected to two H bridges which are then series connected to the three phase grid through a T type multilevel converter which is hereafter referred to as line frequency unfolder. The line frequency unfolder converts the three phase AC voltage to pulsating DC voltages at the terminals uvw. The design parameters of the converter are listed in Table I.

The magnetizing inductance and losses in the system are not considered and all the switches are considered ideal for the simplicity of the converter analysis.

A. Unfolder Modulation

Consider the utility line to neutral voltages defined as,

$$v_{an}(t) = V_p \cos(\theta) \tag{1}$$

$$v_{bn}(t) = V_p \cos\left(\theta - \frac{2\pi}{3}\right) \tag{2}$$

$$v_{cn}(t) = V_p \cos\left(\theta + \frac{2\pi}{3}\right) \tag{3}$$

V_p is the peak value of line to neutral voltage, $\theta = \omega t = 2\pi f t$, where f is the line frequency. The line frequency unfolder is switched six times in a line cycle with the switching sequence shown in Fig.2. The letters in the brackets indicate the connection of the three utility phases (a, b and c) to the terminals u, v and w respectively. The modulation of the

TABLE II
UNFOLDER VOLTAGES IN VARIOUS SECTORS

θ	$\left[\frac{-2\pi}{3},\ \frac{-\pi}{3}\right)$	$\left[\frac{-\pi}{3},\ 0\right)$	$\left[0,\ \frac{\pi}{3}\right)$	$\left[\frac{\pi}{3},\ \frac{2\pi}{3}\right)$	$\left[\frac{2\pi}{3},\ \pi\right)$	$\left[\pi,\ \frac{4\pi}{3}\right)$
v_{uv}	v_{ca}	v_{ac}	v_{ab}	v_{ba}	v_{bc}	v_{cb}
v_{vw}	v_{ab}	v_{cb}	v_{bc}	v_{ac}	v_{ca}	v_{ba}

unfolder results in pulsating voltages v_{uv} and v_{vw} with peak value $\sqrt{3}V_p/2$. The voltage v_{vw} lags the v_{uv} by $\pi/3$ radians. For example, during $\theta \in \left[0, \frac{\pi}{3}\right]$ S_{au}, S_{bv}, S_{cw} are *ON*. Thus, $v_{uv} = v_{ab}$ and $v_{vw} = v_{bc}$.

Accordingly, the operation principle of H bridges 2 and 3 are similar since the input to both the bridges is a pulsating DC voltage with a phase shift. Moreover, the analysis over $\theta \in \left[\frac{-\pi}{3}, \frac{\pi}{3}\right]$ is sufficient owing to the periodicity of the waveforms. Consider the sector $\theta \in \left[\frac{-\pi}{3}, \frac{\pi}{3}\right]$ in Fig.2. The switching functions result in a voltage,

$$v_{uv} = \begin{cases} v_{ac} & ; -\pi/3 \leq \theta < 0 \\ v_{cb} & ; 0 \leq \theta < \pi/3 \end{cases} \tag{4}$$

$$v_{vw} = \begin{cases} v_{ab} & ; -\pi/3 < \theta \leq 0 \\ v_{bc} & ; 0 \leq \theta < \pi/3 \end{cases} \tag{5}$$

The voltages in other sectors can be similarly identified and is shown in Table II. It can be seen from Fig.2 that u is always connected to the *most positive* line-neutral voltage and w is always connected to the *most negative* line-neutral voltage. Thus each of the switches in these legs (S_{ju} and S_{jw}, $j \in \{a, b, c\}$) only need to block unipolar voltage and are switched every $\frac{2\pi}{3}$ radians. However, the switches of the middle leg are switched every $\frac{\pi}{3}$ radians and need to block bidirectional voltage. All the switches need to carry bidirectional current. Thus, a T-type multilevel structure is used for the line frequency unfolder as shown in Fig.1.

B. Modulation of DAB units

The proposed converter enables bidirectional power transfer at any power factor. However, for illustration of the dual active bridge modulation in Fig.2, vehicle to grid (DC to AC) power transfer at unity power factor is considered. In general, the reference currents $\bar{i}_a$, $\bar{i}_b$ and $\bar{i}_c$ (see Fig.1) are given by,

$$\bar{i}_a(t) = I_p \cos(\omega t + \phi) \tag{6}$$

$$\bar{i}_b(t) = I_p \cos\left(\omega t + \phi - \frac{2\pi}{3}\right) \tag{7}$$

$$\bar{i}_c(t) = I_p \cos\left(\omega t + \phi + \frac{2\pi}{3}\right) \tag{8}$$

I_p is the peak of line current and ϕ is the power factor angle. Since the unfolder output waveforms are periodic after every $\frac{2\pi}{3}$, $\theta \in \left[\frac{-\pi}{3}, \frac{\pi}{3}\right]$ is analysed henceforth. During this period, phase a is connected to u and thus the reference current $\bar{i}_u = \bar{i}_a$.

Conventional phase shift modulation is used for synthesizing the currents $\bar{i}_u$ and $\bar{i}_w$. Accordingly, the primary and secondary H-bridges are modulated to produce a square waveform with 50% duty ratio as shown in Fig.3a. A phase shift is given between these waves to carry out the power transfer. For the DAB converter with phase shift square wave modulation with frequency f_s as shown in Fig.3a, the voltages applied across the inductor L are given by,

$$v_L = \begin{cases} V_1 + \frac{V_2}{n} & ; 0 \leq t < \Delta t \\ V_1 - \frac{V_2}{n} & ; \Delta t \leq t < \frac{T_s}{2} \\ -V_1 - \frac{V_2}{n} & ; \frac{T_s}{2} \leq t < \frac{T_s}{2} + \Delta t \\ -V_1 + \frac{V_2}{n} & ; \frac{T_s}{2} + \Delta t \leq t < T_s \end{cases} \tag{9}$$

The inductor current is derived using the following expression,

$$L\frac{di_L}{dt} = v_L(t) \tag{10}$$

Noting that the current waveform has half wave symmetry $i_L(0) = -i_L(T_s/2)$. The currents I_1 and I_2 are given by,

$$I_1 = \frac{-1}{4nLf_s}\left(V_2\delta - V_2 + nV_1\right) \tag{11}$$

$$I_2 = \frac{1}{4nLf_s}\left(V_2 - nV_1 + n\delta V_1\right) \tag{12}$$

The power transferred from port 1 to 2 is,

$$P_{12} = \frac{V_1 V_2}{8nLf_s}\delta\left(2 - \delta\right) \tag{13}$$

where $\Delta t = \delta T_s/4$. Considering the DAB operation between H bridges 1 and 2, $V_1 = V_o$, $V_2 = v_{uv}$. Moreover, the average power at the uv terminal is $P = v_{uv} \times \bar{i}_u$. Thus , the current waveform $\bar{i}_u$ is given by,

$$\bar{i}_u\left(\theta\right) = \frac{V_o}{8nLf_s}\delta\left(2 - \delta\right) \tag{14}$$

The current waveform $\bar{i}_u$ is shaped by varying the phase shift between H bridges 1 and 2, δ_{12} over line cycle as shown in Fig.3. The expression of δ_{12} can be derived from (14) as,

$$\delta_{12}\left(\theta\right) = 1 - \sqrt{1 - \frac{8nLf_s\bar{i}_u\left(\theta\right)}{V_o}} \tag{15}$$

For $\theta \in \left[\frac{-\pi}{3}, \frac{\pi}{3}\right]$, $\bar{i}_u = \bar{i}_a = I_p \cos\left(\omega t + \phi\right)$. For unity power factor operation, the variation of δ_{12} is shown. The phase shift δ_{13} between bridges 1 & 3 can be similarly derived from the reference current $-i_w$.

$$\delta_{13}\left(\theta\right) = 1 - \sqrt{1 + \frac{8nLf_s\bar{i}_w\left(\theta\right)}{V_o}} \tag{16}$$

C. Soft Switching features

Consider the DAB converter operating with conventional phase shift modulation scheme as discussed in the previous section. The switching transition at $t = 0$ is considered to demonstrate capacitor assisted soft switching in Fig.4. The converter is going from negative active state (S_2 and S_3 ON) to

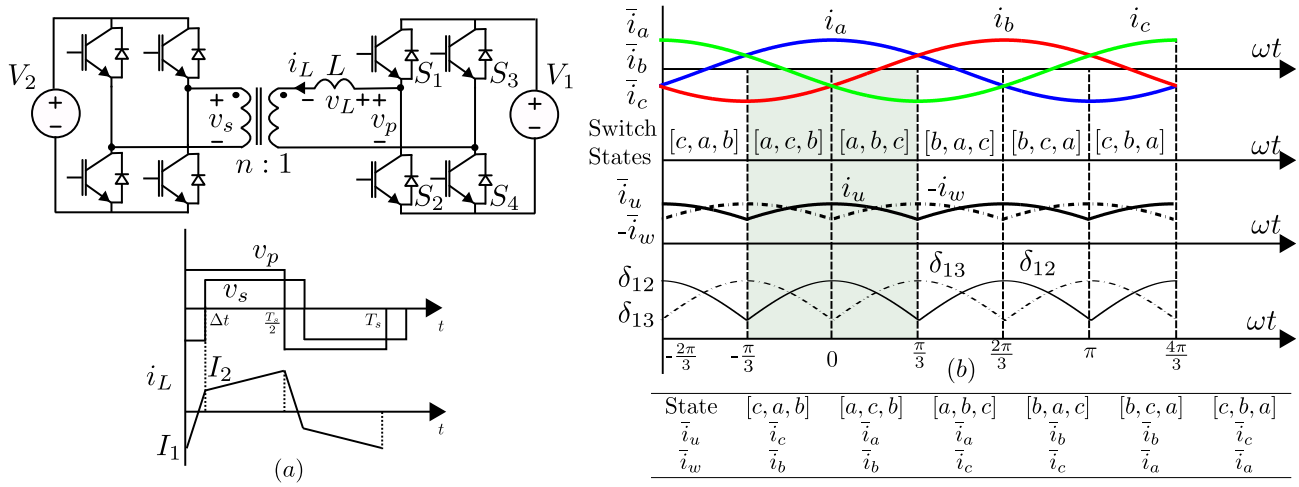

Fig. 3. Waveforms illustrating DAB operation (a) DAB formed by H-bridges 1 and 2 and operating waveforms (b) Operating waveforms for DAB formed by H-bridges 1 and 2 and DAB formed by H-bridges 1 and 3

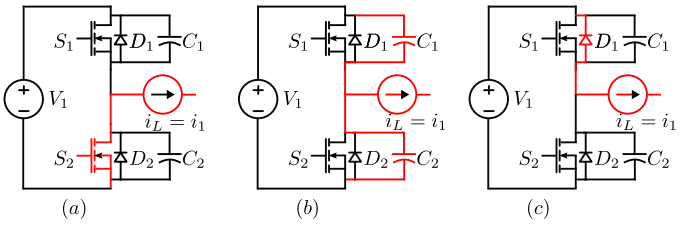

Fig. 4. Capacitor assisted soft turn-off and turn-on

the positive active state (S_1 and S_4 ON). Accordingly, switch S_2 is turned OFF and S_1 is turned on after dead time as shown in Fig.4. Assuming that the current at the instant of turn-off of S_2 to be less than zero, the switch S_2 is conducting prior to its turn-off. This implies $v_{C2} = 0$ (Fig.4a). When switch S_2 is turned off, the current quickly shifts to the capacitors C_1 and C_2 (Fig.4b) and the switch channel is turned off before the voltage across the capacitor can build up implying ZVS. The inductor current discharges the capacitor C_1 and the diode starts conducting once the voltage $v_{C1} = 0$. The switch S_1 is turned on when its body diode is conducting thus resulting in ZVS turn on.

Thus, the current polarity I_1 should be negative to facilitate capacitor assisted soft switching. Similarly, analysing the switching transient at $t = \Delta t$, I_2 should be greater than zero to facilitate soft switching.

For power factor less than 30°, the reference current waveforms $\bar{i}_u$ and $-\bar{i}_w$ are always positive. This means δ_{12} and δ_{13} are always positive and bridge 2 and 3 square waveforms are phase shifted with respect to bridge 1 square waveform. When the Bridge 1 switches at $t = 0$, the sum of bridge 2 and bridge 3 currents needs to be switched.

For the converter operation with the design parameters listed in Table I, the current $I_p = 11.4A$. Accordingly, the values δ_{12} and δ_{13} can be determined using (15) and (16) respectively. The currents at the instants $t = 0$, $\Delta t_{12} = \delta_{12} T_s/4$ and

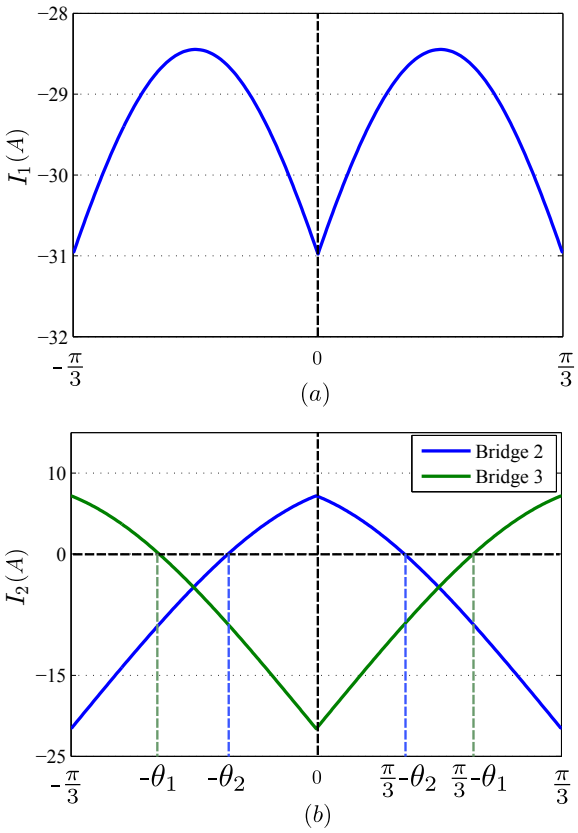

Fig. 5. Current magnitudes at the instant of bridge switching (a) H-Bridge 1 (b) H-Bridge 2 and 3

$\Delta t_{13} = \delta_{13} T_s/4$ can be determined for every switching cycle using (11) and (12). Fig.5 shows the current magnitudes at the instant of bridge 1, 2 and 3 switching. Since the waveforms are periodic after every $\pi/3$, only $\theta \in (-\pi/3, \pi/3)$ is shown. For the leading bridge (H-bridge 1 in the present scenario) to be

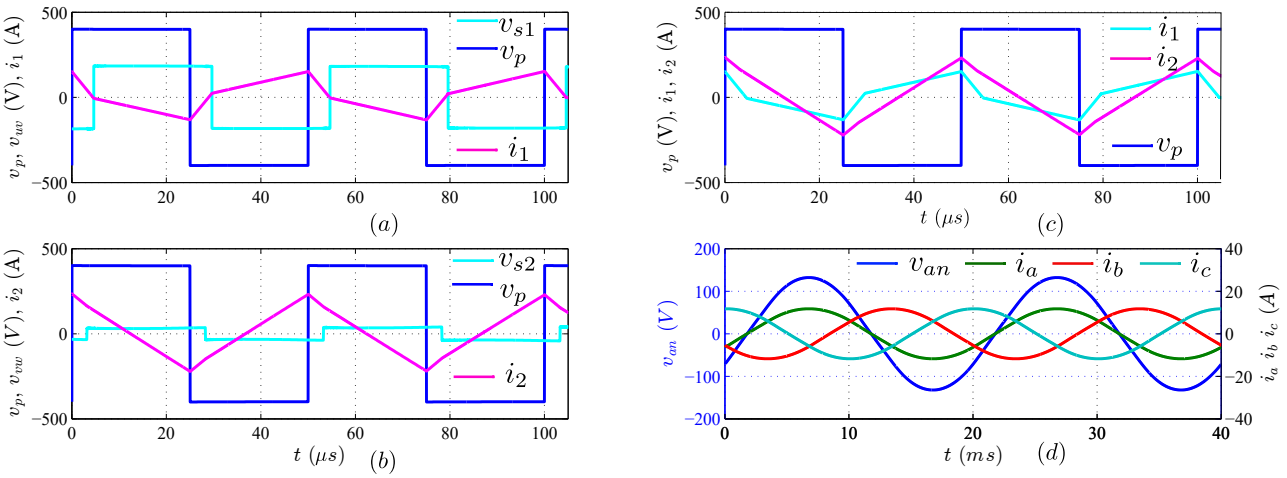

Fig. 6. Simulation Results (a) Switching Cycle Waveforms of DAB formed by H bridge 1 and 2 (currents at 10x) (b) Switching Cycle Waveforms of DAB formed by H bridge 1 and 3 (currents at 10x) (c) DAB Primary voltage and currents in parallel branches (d) v_{an} and i_a in phase confirming UPF operation

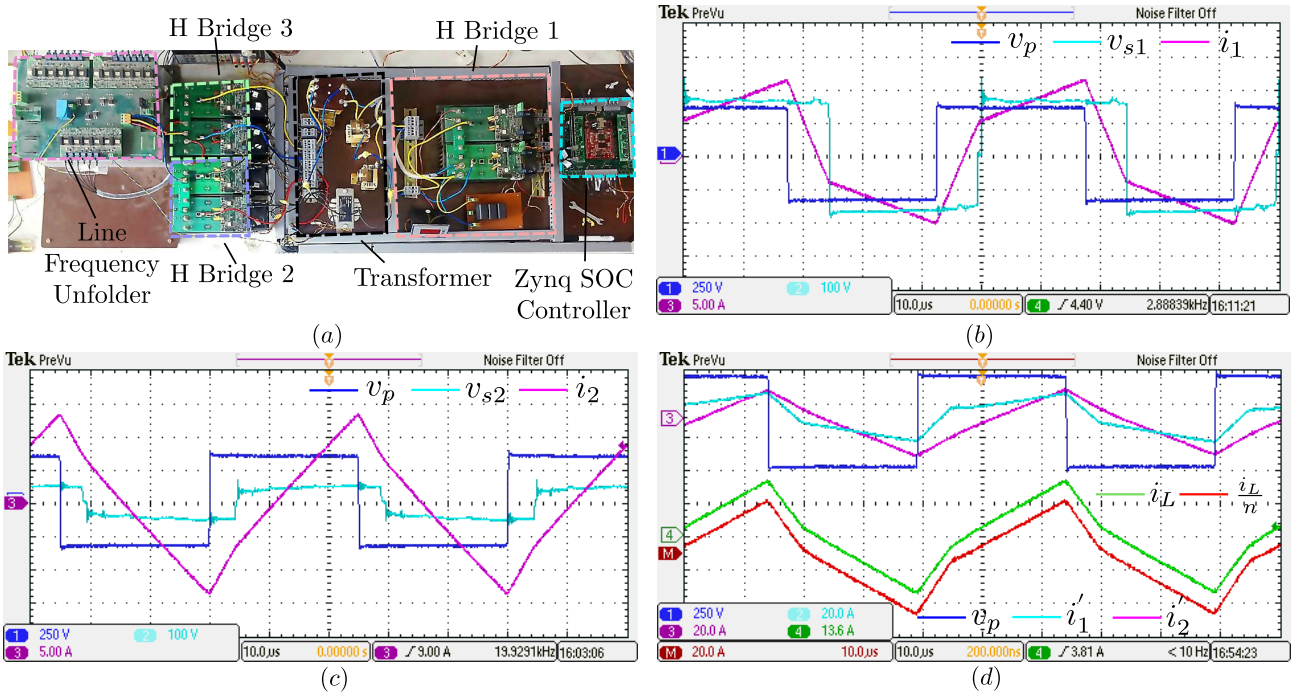

Fig. 7. Experimental Results (a) Hardware Setup (b) Switching Cycle Waveforms of DAB formed by H bridge 1 and 2 (c) Switching Cycle Waveforms of DAB formed by H bridge 1 and 3 (d) H bridge 1 Operation

soft switched, the current at the switching instant $t = 0$ should be *negative*. It can be seen from Fig.5a that, H-bridge-1 always switches at $t = 0$ with negative current. This implies that the primary side H-bridge is soft switched over the entire line cycle. ZVS happens in Bridges 2 and 3 when the current during switching at $t = \Delta t$ is *positive*. Bridge 2 current is positive only during $\theta \in \left(-\theta_2, \frac{\pi}{3} - \theta_2\right)$ Thus ZVS happens only in the aforesaid region which repeats after every $\pi/3$. Similarly Bridge 3 is soft switched for $\theta \in \left(-\frac{\pi}{3}, -\theta_1\right) \cup \left(\frac{\pi}{3} - \theta_1, \frac{\pi}{3}\right)$. Thus partial ZVS happens for AC side H-bridges in certain sections of the line cycle.

III. Simulation and Experimental Results

The proposed converter topology and modulation strategy was simulated in MATLAB with the parameters described in Table I and DC to AC power flow.

Fig.6a shows the operating waveforms for a switching cycle for the DAB unit formed by H bridges 1 and 2. It can be seen that the inductor current varies linearly according to the voltages v_p and v_{uv}. Similar behaviour is observed for the DAB unit formed by H bridges 1 and 3 (Fig.6b). Fig.7c shows the operation of the primary H-bridge at a given instant in the line cycle ($\theta = \pi/18$). The different current slopes

indicate that both the DAB units are performing with non-identical phase shifts as desired. Fig.6d shows the phase A line to neutral voltage along with the three phase currents. The currents are balanced and i_a is in phase with v_{an} confirming UPF operation. The system was simulated at a power level of 2.1 kW which corresponds to a line current peak of 11.3 A. This can be verified from Fig.6d. The experimental switching cycle waveforms for the dual active bridge units are shown in Fig.7b and c. The primary voltage and the secondary currents for a given switching instant are shown in Fig.7d. The sum of the transformer currents $i_1^{'}$ and $i_2^{'}$ calculated using math operation is shown in red. This sum has exact resemblance to i_L and is scaled by turns ratio n.

IV. Conclusion

This paper presented a novel single stage converter topology and modulation that can enable bidirectional power flow. Use of line frequency unfolding scheme enables low switching losses. Use of DAB conversion technique reduces the switching losses through soft switching. It is observed that use of the proposed modulation strategy results in the primary side H-bridge to be completely soft-switched. However, secondary side H-bridges working with pulsating DC voltages are partially soft switched in certain sections of the line cycle.

References

[1] M. Yilmaz and P. T. Krein, "Review of battery charger topologies, charging power levels, and infrastructure for plug-in electric and hybrid vehicles," *IEEE Transactions on Power Electronics*, vol. 28, no. 5, pp. 2151–2169, May 2013.

[2] U. R. Prasanna, A. K. Singh, and K. Rajashekara, "Novel bidirectional single-phase single-stage isolated AC-DC converter with PFC for charging of electric vehicles," *IEEE Transactions on Transportation Electrification*, vol. 3, no. 3, pp. 536–544, Sept 2017.

[3] S. Li, J. Deng, and C. C. Mi, "Single-stage resonant battery charger with inherent power factor correction for electric vehicles," *IEEE Trans. Veh. Technol.*, vol. 62, no. 9, pp. 4336–4344, Nov 2013.

[4] D. Patil and V. Agarwal, "Compact onboard single-phase EV battery charger with novel low-frequency ripple compensator and optimum filter design," *IEEE Trans. Veh. Technol.*, vol. 65, no. 4, pp. 1948–1956, April 2016.

[5] A. Pal and K. Basu, "A soft-switched high frequency link single-stage three-phase inverter for grid integration of utility scale renewables," *IEEE Transactions on Power Electronics*, pp. 1–1, 2018.

[6] W. W. Chen, R. Zane, and L. Corradini, "Isolated bidirectional grid-tied three-phase ac–dc power conversion using series-resonant converter modules and a three-phase unfolder," *IEEE Transactions on Power Electronics*, vol. 32, no. 12, pp. 9001–9012, Dec 2017.

[7] R. W. A. A. D. Doncker, D. M. Divan, and M. H. Kheraluwala, "A three-phase soft-switched high-power-density dc/dc converter for high-power applications," *IEEE Trans. Ind. Appl.*, vol. 27, no. 1, pp. 63–73, Jan 1991.

[8] H. Bai and C. Mi, "Eliminate reactive power and increase system efficiency of isolated bidirectional dual-active-bridge dc-dc converters using novel dual-phase-shift control," vol. 23, no. 6, pp. 2905–2914, 2008.

[9] M. A. Sayed, K. Suzuki, T. Takeshita, and W. Kitagawa, "Soft-switching PWM technique for grid-tie isolated bidirectional DC-AC converter with SiC device," *IEEE Trans. Ind. Appl.*, vol. 53, no. 6, pp. 5602–5614, Nov 2017.

[10] N. D. Weise, G. Castelino, K. Basu, and N. Mohan, "A single-stage dual-active-bridge-based soft switched AC/DC converter with open-loop power factor correction and other advanced features," *IEEE Trans. Power Electron.*, vol. 29, no. 8, pp. 4007–4016, Aug 2014.

[11] R. Baranwal, K. V. Iyer, K. Basu, G. F. Castelino, and N. Mohan, "A reduced switch count single-stage three-phase bidirectional rectifier with high-frequency isolation," *IEEE Trans. on Power Electron.*, vol. 33, no. 11, pp. 9520–9541, Nov 2018.

[12] D. Das, N. Weise, K. Basu, R. Baranwal, and N. Mohan, "A bidirectional soft-switched DAB-based single-stage three-phase ac–dc converter for V2G application," *IEEE Transactions on Transportation Electrification*, vol. 5, no. 1, pp. 186–199, March 2019.